

Anomalous charge-, spin-, and lattice-dynamics in the charge-ordered phase of $\text{Bi}_{1-x}\text{Ca}_x\text{MnO}_3$ ($x > 0.5$)

S. Yoon¹, M. Rübhausen¹, S. L. Cooper¹, K. H. Kim^{2,3}, and S-W. Cheong^{2,4}

¹*Department of Physics and Frederick Seitz Materials Research Laboratory,
University of Illinois at Urbana-Champaign, Urbana, IL 61801*

²*Department of Physics and Astronomy, Rutgers University, Piscataway, NJ 08854*

³*Department of Physics, Seoul National University, Seoul 151-742, Korea*

⁴*Bell Laboratories, Lucent Technologies, Murray Hill, NJ 07974*

(December 2, 2024)

We report an inelastic light scattering study of the effects of charge-ordering on the charge-, lattice-, and spin-dynamics in $\text{Bi}_{1-x}\text{Ca}_x\text{MnO}_3$ ($x > 0.5$). We show that charge-ordering results not only in anomalous phonon behavior, such as the appearance of ‘activated’ modes, but more significantly in the appearance of a quasielastic scattering response of distinctive T_{1g} symmetry, indicative of magnetic fluctuations associated with ‘chiral’ charge motion in the CO/AFM phase.

PACS numbers: 78.30.-j, 75.30.-m

Among the most interesting and rich phenomena exhibited by complex transition metal oxides such as the nickelates [1], cuprates [2], and manganites [3] is charge- and orbital-ordering, i.e., the organization of charges and orbital configurations in periodic arrays on the lattice. The considerable recent effort devoted to understanding this behavior has revealed a variety of interesting properties, including novel states of matter such as co-existing magnetic phases [4,5] and possible ‘quantum liquid crystal’ states [6]. Yet, a number of important issues remain unsolved, including the manner in which ferromagnetic and antiferromagnetic correlations compete to generate the diversity of magnetic phases in these systems, the process by which polarons self-organize in the charge-ordered (CO) phase, the effects of long-range charge/orbital ordering on lattice and charge dynamics, and the nature of carrier motion through the antiferromagnetic spin background of the Néel state. A clarification of these issues demands experimental methods capable of probing the strong interplay among the spin-, charge-, lattice-, and orbital-degrees-of-freedom in strongly-correlated systems.

In this Letter, we discuss an inelastic light (Raman) scattering study of the unconventional lattice-, spin-, and charge-dynamics in the CO phase of the $\text{Bi}_{1-x}\text{Ca}_x\text{MnO}_3$ ($x > 0.5$) system. Raman scattering offers several unique features in the investigation of charge-ordered systems: (a) by providing energy, symmetry, and lifetime information concerning lattice-, spin-, as well as charge-excitations, Raman scattering affords unique insight into the interplay among these coupled excitations in various phases; (b) as an optical probe that can be easily focused onto individual CO domains, polarized Raman scattering can give important information regarding the anisotropic lattice and charge dynamics in the CO phase; and (c) as a technique that can convey information about carrier dynamics, and even about exotic “chiral” charge currents

[7,8], Raman scattering offers a means of probing the unconventional nature of carrier motion in the complex spin environment of the Néel state in CO systems.

All of these benefits are clearly evident in the present study, which uncovers several interesting features of CO behavior in $\text{Bi}_{1-x}\text{Ca}_x\text{MnO}_3$ ($x > 0.5$). First, polarized Raman measurements show that charge-ordering results in the appearance of activated phonon modes, due to the lowering of symmetry by charge-stripe formation, and also in the development of an anisotropy between the lattice dynamics along, and perpendicular to, the charge-stripe direction. Even more interesting, with decreasing temperature into the CO phase, these studies reveal the development of a quasielastic Raman scattering response with distinctive T_{1g} symmetry. This indicates the presence of strong magnetic fluctuations in the CO/AFM phase, caused by closed-loop (“chiral”) charge currents arising from the strong constraints placed on conduction by the complex spin-texture of the Néel state and the double-exchange hopping mechanism.

The samples used in our study were flux-grown single crystalline $\text{Bi}_{0.19}\text{Ca}_{0.81}\text{MnO}_3$ ($T_{\text{co}} = T_{\text{N}} = 165$ K) and $\text{Bi}_{0.18}\text{Ca}_{0.82}\text{MnO}_3$ ($T_{\text{co}} = 210$ K, $T_{\text{N}} = 160$ K). The typical dimensions of these samples are $2 \times 2 \times 1$ mm³. Raman spectra were measured in a backscattering geometry using continuous helium flow and cold-finger optical cryostats, and a modified subtractive-triple-grating spectrometer equipped with a nitrogen-cooled CCD array detector. The spectra were corrected for the spectral response of the spectrometer and the detector. The samples were excited with 4 mW of the 4762-Å line of the Kr⁺ laser, focused to a 50 μm diameter spot within a single CO domain of the crystals. Temperatures listed for the Raman spectra include estimates of laser heating effects. To identify excitation symmetries, the spectra were obtained with the incident (\mathbf{E}_i) and scattered (\mathbf{E}_s) light polarized in various configurations, including ($\mathbf{E}_i, \mathbf{E}_s$) =

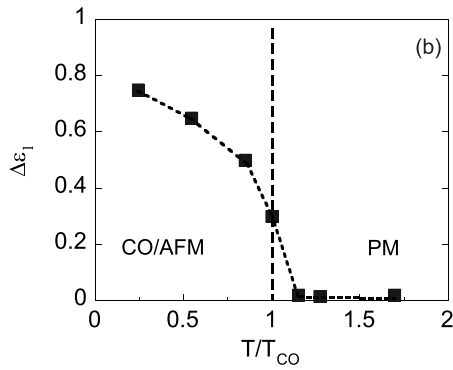
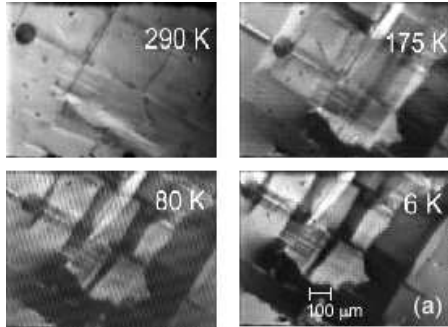


FIG. 1. (a) Polarized microscope images of developing CO domains at various temperatures. (b) Dielectric anisotropy parameter $\Delta\epsilon_1$ (see text) at $\omega = 1$ eV. The dotted line is a guide to the eye.

(**x,x**) and (**y,y**): $A_{1g} + E_g$, and (**E_i, E_s**) = (**L,L**): $A_{1g} + \frac{1}{4}E_g + T_{1g}$, where x and y are the [100] and [010] crystal directions, respectively, L is left circular polarization, and where A_{1g} , E_g and T_{1g} are respectively the singly-, doubly-, and triply-degenerate irreducible representations of the O_h space group of the crystals, which have a pseudocubic structure [15].

Figure 1 (a) shows polarized microscope images of the (100) $\text{Bi}_{0.19}\text{Ca}_{0.81}\text{MnO}_3$ sample surface taken at 290 K, 175 K, 80 K, and 6 K, respectively. One can clearly see the growth of “light” and “dark” regions below the charge-ordering temperature, $T_{\text{co}} = 165$ K, corresponding to the development of domains having perpendicular orientations of the charge-stripes. Interestingly, a remnant of the domains can be seen even above the charge-ordering temperature at $T = 175$ K, perhaps indicative of charge-stripe fluctuations above T_{co} . The evolution of CO behavior and domain formation below T_{co} is more quantitatively illustrated in Fig. 1 (b), which presents the temperature dependence of the dielectric anisotropy, $\Delta\epsilon_1(\omega) = \frac{|\epsilon_1^{ac} - \epsilon_1^{bc}|}{\sqrt{(\epsilon_1^{ac})^2 + (\epsilon_1^{bc})^2}}$, where ϵ_1^{ac} and ϵ_1^{bc} are the dielectric responses for $\omega = 1$ eV light polarized in the ac and bc planes respectively [16].

Two points of particular interest can be made regarding the dielectric anisotropy $\Delta\epsilon_1$ in Fig. 1 (b). First, the temperature-dependence of $\Delta\epsilon_1$ is similar to that of the order-parameter in a second-order phase transition, consistent with our expectation that the increasing size

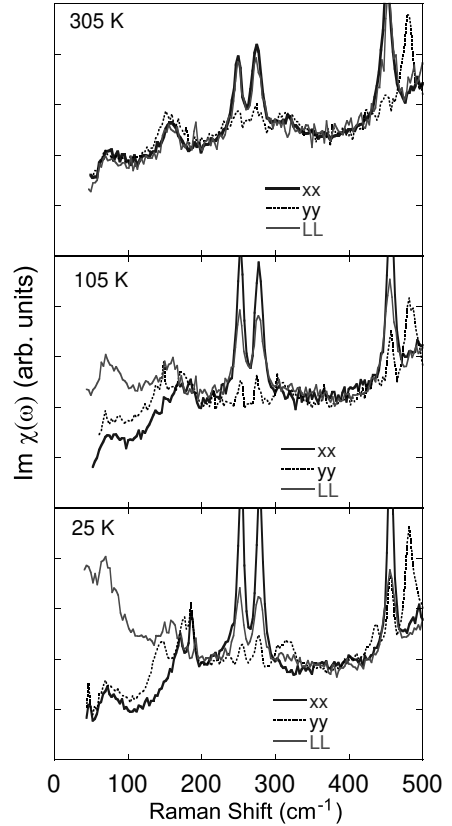


FIG. 2. Raman spectra of $\text{Bi}_{0.19}\text{Ca}_{0.81}\text{MnO}_3$ in xx, yy and LL polarization configurations at 305 K, 105 K, and 25 K.

of this quantity below T_{co} reflects the increasing organization of charges below T_{co} . However, at low temperatures, $\Delta\epsilon_1$ saturates below the maximum value of 1 due to the fact that the optical spot in the ellipsometry measurements is not isolated to a single domain. This illustrates one of the distinct advantages of polarized Raman scattering techniques for measuring optical anisotropy in the CO phase, as this technique allows the study of single ($\lesssim 100$ μm) domains with uniformly aligned charge stripes.

Raman spectra of single domain regions in $\text{Bi}_{0.19}\text{Ca}_{0.81}\text{MnO}_3$ are illustrated, for various temperatures and scattering geometries, in Fig. 2. Note first that in the high temperature “isotropic” phase ($T = 305$ K), all three scattering geometries (xx, yy, and LL) overlap, with the exception of some intensity differences associated with the phonons. However, with decreasing temperature into the CO phase, two significant features are evident: First, several changes in the phonon spectra evolve with decreasing temperature, including the appearance of new modes and the evolution of differences in the phonon spectra associated with the xx and yy scattering geometries. Second, while the low frequency backgrounds associated with the xx and yy scattering geometries decrease with decreasing temperature into the CO phase, there is a dramatic growth of the

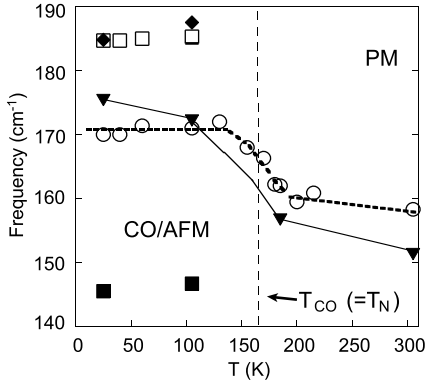


FIG. 3. Hardening of the Mn vibration mode ($\sim 160 \text{ cm}^{-1}$) and the development of additional modes ($\sim 145 \text{ cm}^{-1}$ and $\sim 185 \text{ cm}^{-1}$) below the CO transition. Open symbols denote data from xx, and filled symbols denote data from yy scattering geometries. The lines are guides to the eye.

low frequency scattering background in the LL geometry, betraying the development of a distinctive T_{1g} -symmetry quasielastic scattering response in the CO/AFM phase.

We focus first on the effects of charge-ordering on the phonons in $\text{Bi}_{0.19}\text{Ca}_{0.81}\text{MnO}_3$ - such information is important, as the optical phonons function as ‘local probes’ of changes in the local symmetry and bond-strengths caused by charge-ordering. Consider first the $\sim 160 \text{ cm}^{-1} A_{1g}$ phonon mode denoted by circles and triangles in Fig. 3, which is likely to be associated with in-phase Mn vibrations. This mode exhibits an abrupt hardening across the charge-ordering transition, indicative of the effects of charge-ordering on the lattice force constants via changes in the Coulomb energies. Also, Fig. 3 shows that a second mode at $\sim 185 \text{ cm}^{-1}$, which in the isotropic high temperature phase is present in the xy scattering configuration, appears in the xx scattering geometry below the charge-ordering temperature due to the consequent breakdown of symmetry selection rules.

The breaking of 4-fold in-plane symmetry due to long-range charge-ordering is also reflected in differences in the phonon spectra observed in the xx and yy scattering geometries. In particular, the yy spectrum at 25 K (Fig. 2) shows the development of ‘new’ phonon modes near $\sim 145 \text{ cm}^{-1}$ (filled squares in Fig. 3), $\sim 300 \text{ cm}^{-1}$, and $\sim 420 \text{ cm}^{-1}$. The appearance of new modes possibly reflects Brillouin-zone-folding of zone boundary modes to the zone center, caused by the additional periodicity associated with charge-stripe formation. It is expected, however, that zone-folded modes should have much weaker intensities than ‘regular’ modes [19,20], which is not the present case. A more plausible interpretation therefore is that the new modes are “activated” modes due to charge-ordering: For example, the out-of-phase Mn vibrational mode is not Raman-active in the PM ‘isotropic’ phase because the net charge fluctuation associated with out-of-phase motion of the $(\text{Mn}^{3.5+} - \text{O} - \text{Mn}^{3.5+})$ complex is zero, and hence this mode cannot modulate the polar

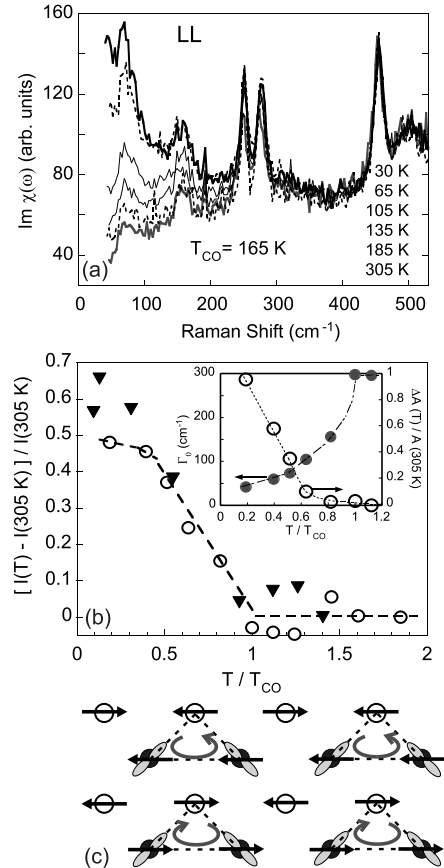


FIG. 4. (a) Temperature dependence of the Raman spectra in the LL scattering geometry. (b) Fractional change in the integrated quasielastic Raman scattering intensity ($50 - 350 \text{ cm}^{-1}$) as a function of temperature for the $T_{\text{co}} = 165 \text{ K}$ (circles) and $T_{\text{co}} = 210 \text{ K}$ (triangles) samples. Inset: Fractional change in the quasielastic scattering amplitude A and fluctuation rate Γ as a function of temperature. Lines are guides to the eye. (c) ‘Chiral’ motion of holes in the C-type spin CO/AFM phase, illustrated for $x = 0.5$. Filled and empty circles represent Mn^{3+} and Mn^{4+} sites, respectively.

izability. However, in the CO phase, the different charges on the Mn^{3+} and Mn^{4+} sites cause out-of-phase Mn vibrations of the $(\text{Mn}^{3+} - \text{O} - \text{Mn}^{4+})$ complex to have a non-zero net charge fluctuation that couples to the polarizability, resulting in the ‘new’ Raman-active mode at 145 cm^{-1} .

An even more interesting feature apparent in Figs. 2 and 4 (a) is the development in the CO state of a quasielastic Raman response in the LL scattering geometry,

$$\text{Im}\chi(\omega) \sim \frac{A\omega\Gamma}{\omega^2 + \Gamma^2} \quad (1)$$

where A is the quasielastic scattering amplitude and Γ is the fluctuation rate. The absence of a similar scattering response in either xx or yy configurations identifies this quasielastic response as having primarily T_{1g} symmetry. This distinctive scattering symmetry transforms

like both the spin-chirality ($\vec{S}_1 \cdot \vec{S}_2 \times \vec{S}_3$) [21] and magnetic dipole operators, and is typical of scattering from magnetic fluctuations [22]. Thus, while the ground state of the CO/AFM phase is not generally expected to have a net magnetization or spin chirality, the development of this T_{1g} quasielastic response in Figs. 2 and 4 (a) betrays the presence of strong fluctuations associated with such a broken symmetry state in the CO/AFM phase.

When considering the origin of this anomalous scattering response, we can first rule out a “precursor” fluctuational response associated with either charge-stripe- or orbital-ordering: while such responses should develop above, become maximum near, and diminish below the ordering transition temperature T_{co} , Figs. 4 (a) and (b) clearly illustrate that the T_{1g} quasielastic response we observe evolves at T_{co} , and grows with decreasing temperature below T_{co} , coincident with the charge-order-parameter Δ^{ϵ_1} in Fig. 1 (b). We can also likely rule out spin fluctuations associated with a canted AFM phase, as neutron scattering studies show no evidence for ferromagnetic spin fluctuations below T_N in this system [15].

An intriguing possibility consistent with both the distinctive T_{1g} symmetry and temperature dependence of the quasielastic light scattering response in Figs. 4 (a) and (b) is that it is associated with a fluctuational response arising from chiral charge currents, i.e., charges constrained to hop in triangular loops. The propensity for such chiral charge motion in the “type C” spin environment of the CO/AFM phase (see Fig. 4 (c)) can be seen by first noting that *translational* charge motion is strongly limited in this phase by three principal effects: the complex orbital and Néel spin texture, the constraints of the double-exchange hopping mechanism, and disorder (e.g., by doping away from commensurate fillings), which strongly limits conduction along the 1D Mn^{3+} chains [23]. However, Fig. 4 (c) illustrates that the hopping of holes in triangular plaquettes is not constrained by either the spin or orbital environments in this CO/AFM phase, and therefore the scattering intensity associated with this conduction path should evolve below T_{co} concomitant with the development of the Néel ordered state. Interestingly, Nagaosa and Lee predicted that such “closed-loop” charge hopping should be present in doped AFM insulators, and should be manifest in the appearance of an additional quasielastic Raman response [8] similar to that observed in the CO/AFM phase of $Bi_{1-x}Ca_xMnO_3$ ($x > 0.5$) (Fig. 4 (a)). Such quasielastic light scattering arises from fluctuations in an induced effective magnetic field generated by the chiral charge currents, $\langle \chi(m)\chi^\dagger(m) \rangle \sim \langle mm^\dagger \rangle$, where $\chi(m)$ is the ‘field’-dependent electric susceptibility.

The possible presence of chiral charge currents in the CO/AFM phase of $Bi_{1-x}Ca_xMnO_3$ ($x > 0.5$) suggests

that this phase may be an interesting regime in which to explore the exotic transport properties of doped AFM insulators [8], particularly in view of the rich interplay that exists among band-filling, Néel ordering, and electron-lattice coupling in CO systems. Further, these results raise numerous questions concerning possible chiral charge hopping in CO/AFM materials, such as the effects of filling and decreasing temperature, and the influence of chiral charge hopping in the CO phase on other measurements such as anomalous Hall effect [24] and noise measurements.

We thank M. V. Klein, Y. Lyanda-Geller, and P. Goldbart for useful discussions. We acknowledge financial support of the DOE via DEFG02-96ER45439 (S.Y., M.R., S.L.C.), the DFG via Ru 773/1-1, the NSF through the STCS via DMR91-20000 (M.R.), and NSF-DMR-9802513 (K.H.K., S-W.C.).

- [1] C. H. Chen *et al.*, Phys. Rev. Lett. **71**, 2461 (1993).
- [2] J. M. Tranquada *et al.*, Nature (London) **375**, 561 (1995).
- [3] C. H. Chen *et al.*, Phys. Rev. Lett. **76**, 4042 (1996).
- [4] H. L. Liu, S. L. Cooper, and S-W. Cheong, Phys. Rev. Lett. **81**, 4684 (1998).
- [5] A. Moreo, S. Yunoki, and E. Dagotto, Science **283**, 2034 (1999).
- [6] S. A. Kivelson, E. Fradkin, and V. J. Emery, Nature (London) **393**, 550 (1998).
- [7] D. V. Khveshchenko and P. B. Wiegmann, Phys. Rev. Lett. **73**, 500 (1994).
- [8] N. Nagaosa and P. A. Lee, Phys. Rev. B **43**, 1233 (1991).
- [9] H. Y. Hwang *et al.*, Phys. Rev. B **52**, 15046 (1995).
- [10] Y. Moritomo *et al.*, Phys. Rev. B **55**, 7549 (1997).
- [11] S. Mori, C. H. Chen, and S-W. Cheong, Nature (London) **392**, 473 (1998).
- [12] P. G. Radaelli *et al.*, Phys. Rev. B **55**, 3015 (1997).
- [13] P. Schiffer *et al.*, Phys. Rev. Lett. **75**, 3336 (1995).
- [14] A. P. Ramirez *et al.*, Phys. Rev. Lett. **76**, 4042 (1996).
- [15] W. Bao *et al.*, Phys. Rev. Lett. **78**, 543 (1997).
- [16] M. Rübhausen *et al.*, submitted to Phys. Rev. B.
- [17] M. N. Iliev *et al.*, Phys. Rev. B **57**, 2872 (1998).
- [18] K. Yamanoto *et al.*, J. Phys. Soc. Jpn **68**, 2538 (1999).
- [19] E. Ya. Sherman *et al.*, Europhys. Lett. **48**, 648 (1999).
- [20] M. Fischer, *et al.*, Phys. Rev. B **60**, 7284 (1999).
- [21] B. S. Shastry and B. I. Shraiman, Phys. Rev. Lett. **65**, 1068 (1990).
- [22] S. L. Cooper *et al.*, Phys. Rev. B **35**, 2615 (1987); S. L. Cooper *et al.*, *ibid.*, **36**, 5743 (1987).
- [23] R. Maezono *et al.*, Phys. Rev. B **57**, R13993 (1998).
- [24] S. H. Chun *et al.*, Phys. Rev. Lett. **84**, 757 (2000); Y. Lyanda-Geller *et al.*, cond-matt/9904331; J. Ye *et al.*, Phys. Rev. Lett. **83**, 3737 (1999).